

Theoretical investigation on the H sublattice in CaH_6 and energetic performance

Zhihong Huang(黄植泓), Nan Li(李楠), Jun Zhang(张俊), Xiuyuan Li(李修远), Zihuan Peng(彭梓桓), Chongwen Jiang(江崇文), and Changqing Jin(靳常青)

Citation: Chin. Phys. B, 2025, 34 (**8**): 086202. DOI: 10.1088/1674-1056/ade1c3
http://cpb.iphy.ac.cn; http://iopscience.iop.org/cpb

What follows is a list of articles you may be interested in

Band gap engineering and vibrational properties of van der Waals semiconductor $ZnPSe_3$ under compression

Rouqiong Su(苏柔琼), Yuying Li(李玉莹), Chunhua Chen(陈春华), Yifang Yuan(袁亦方), and Haizhong Guo(郭海中)

Chin. Phys. B, 2025, 34 (**6**): 066205. DOI: 10.1088/1674-1056/adcaa2

Structural regulation and optical behavior of zero-dimensional Cu(I)-based organometallic halides under pressure

Runnan Ye(叶润楠), Jingtian Wang(王敬天), Jiayi Yang(杨佳毅), Xuchen Wang(王旭晨), Junce Lei(雷钧策), Wenya Zhao(赵文雅), Yufan Meng(孟雨凡), Guanjun Xiao(肖冠军), and Bo Zou(邹勃)

Chin. Phys. B, 2025, 34 (**6**): 066204. DOI: 10.1088/1674-1056/adc193

Bulk modulus of molecular crystals

Xudong Jiang(江旭东), Yajie Wang(汪雅洁), Kuo Li(李阔), and Haiyan Zheng(郑海燕)

Chin. Phys. B, 2025, 34 (**6**): 066201. DOI: 10.1088/1674-1056/adca1a

Stoichiometric change and solid decomposition in Ca-S compounds under high pressure

Yang Lv(吕阳), Jian-Fu Li(李建福), Zhao-Bin Zhang(张钊彬), Yong Liu(刘勇), Jia-Nan Yuan(袁嘉男), Jia-Ni Lin(林佳妮), and Xiao-Li Wang(王晓丽)

Chin. Phys. B, 2025, 34 (**4**): 046202. DOI: 10.1088/1674-1056/adb38e

Electronic structure and phase transition engineering in NbS_2: Crucial role of van der Waals interactions

Wei Wang(王威), Wen Lei(雷文), Xiaojun Zheng(郑晓军), Huan Li(黎欢), Xin Tang(唐鑫), Xing Ming(明星)

Chin. Phys. B, 2020, 29 (**5**): 056201. DOI: 10.1088/1674-1056/ab8214

SPECIAL TOPIC — Structures and properties of materials under high pressure

Theoretical investigation on the H sublattice in CaH_6 and energetic performance

Zhihong Huang(黄植泓)[1], Nan Li(李楠)[1,†], Jun Zhang(张俊)[2,‡], Xiuyuan Li(李修远)[1], Zihuan Peng(彭梓桓)[1], Chongwen Jiang(江崇文)[1], and Changqing Jin(靳常青)[2]

[1] *State Key Laboratory of Explosion Science and Technology, School of Mechatronical Engineering, Beijing Institute of Technology, Beijing* 100081, *China*
[2] *Beijing National Laboratory for Condensed Matter Physics, Institute of Physics, Chinese Academy of Sciences, Beijing* 100190, *China*

(Received 16 April 2025; revised manuscript received 3 June 2025; accepted manuscript online 6 June 2025)

Metal superhydride compounds (MSHCs) have attracted much attention in the fields of high-pressure physics due to the superconductivity properties deriving from the metallic-hydrogen-like characteristics and relatively mild synthesis conditions. However, their energetic performance and related potential applications are still open issues till now. In this study, CaH_6 and NbH_3, which exhibit evidently differences in their geometric and electronic structures, were chosen as examples of MSHCs to investigate their energetic performance. The structure, bonding features and energetic performance of CaH_6 and NbH_3 were predicted based on first-principles calculations. Our results reveal that high-pressure MSHCs always exhibit high energy densities. The range of theoretical energy density of CaH_6 was predicted as 2.3–5.3 times of TNT, while the value for NbH_3 was predicted as 1.2 times of TNT. Our study further uncover that CaH_6 has outstanding energetic properties, which are ascribed to the three-dimensional (3D) aromatic H sublattice and the strong covalent bonding between the H atoms. Moreover, the detonation process and products of rapid energy-release stage of CaH_6 were simulated via AIMD method, based on which its superior combustion performance was predicted and its specific impulse was calculated as 490.66 s. This study not only enhances the chemical understanding of MSHCs, but also extends the paradigm of traditional energetic materials and provides a new route to design novel high energy density materials.

Keywords: metal superhydride compounds, energetic performance, first-principles simulation, high pressure

PACS: 62.50.–p, 63.90.+t, 65.40.–b, 71.15.Pd

DOI: 10.1088/1674-1056/ade1c3 **CSTR:** 32038.14.CPB.ade1c3

1. Introduction

Metallic hydrogen has long been sought in the field of high-pressure physics since its first proposal in 1935 by physicists Eugene Wigner and Hillard Huntington,[1] with numerous theoretical studies revealing its outstanding properties continuously. In 1968, Ashcroft[2] predicted that metallic hydrogen could exhibit superconductivity at room temperature. In 1999, Nellis[3] predicted its extremely high energy density, making it a potential candidate for fuel, propellant, or explosive. In 2010, its energy density was predicted as 216 MJ/kg by Silvera *et al.*,[4] which is 46.85 times that of trinitrotoluene (TNT) and far exceeds those of widely studied energetic materials such as the most powerful energetic materials hexanitrohexaazaisowurtzitane (CL-20) and 1,3,5,7-tetranitro-1,3,5,7-tetrazocane (HMX). These remarkable predicted properties have propelled the studies of metallic hydrogen to the cutting edge of materials science and high-pressure physics. However, due to the extremely high pressures required, the synthesis and stabilization of metallic hydrogen remain persistent challenges. In 2012, McMahon *et al.*[5] theoretically predicted that the synthesis pressure of metallic hydrogen reaches $\sim$ 500 GPa. In 2017, Isaac Silvera *et al.*[6] reported the observation of metallic hydrogen under approximately 495 GPa, though great controversies remain.

In 2004, Neils[7] proposed the concept of chemical precompression, which could lower the formation pressures of metallic hydrogen by introducing other elements, particularly metals. Following this idea, in 2014, Duan *et al.*[8] predicted that H_3S could be synthesized under 111 GPa, which was regarded as a milestone of superhydrides and proved by experimental success that H_3S was successfully synthesized under 90 GPa in 2015 by MI Eremets.[9] Then, scientists have devoted their research to superhydrides, especially metal superhydride compounds (MSHCs), and more and more novel MSHCs have been achieved.[10–13] Typically, LaH_{10} and CaH_6 exhibit superconductivity with high-T_c higher than 200 K, similar to that predicted for pure solid-state metallic hydrogen.[11,12] Also, the lattices of superhydrides composed of metals near the s–d border and H atoms possess strong covalent H–H networks,[14,15] which inspire us to hypothesize their high energy density. On the other hand, the ambient-pressure metal hydrides such as AlH_3 and MgH_2 have been widely in-

†Corresponding author. E-mail: leen04@bit.edu.cn
‡Corresponding author. E-mail: zhang@iphy.ac.cn

© 2025 Chinese Physical Society and IOP Publishing Ltd. All rights, including for text and data mining, AI training, and similar technologies, are reserved.

vestigated as energetic materials.[16–19] In 2021, Wu *et al.*[17] measured the combustion heat of MgH_2, TiH_2, and ZrH_2 with values of 29.96 MJ/kg, 20.94 MJ/kg, and 12.22 MJ/kg, respectively. In 2024, Makhov *et al.*[19] reported the addition of Al and AlH_3 to an explosive could greatly improve its heat and the TNT equivalent of an underwater explosion. Considering these two aspects, MSHCs should be promising candidates for energetic materials.

In recent years, our research team has synthesized a series of hydrogen-rich MSHCs,[20–22] such as CaH_6 and Lu_4H_{23}, using the diamond anvil cell combined with an *in-situ* laser heating technique. Nevertheless, existing studies[23–26] on high-pressure MSHCs have predominantly focused on their superconductivity and electron–phonon coupling interactions. To date, their energetic performance has barely been studied, while its comprehension is essential for developing novel energetic materials.

In this work, the detailed energetic performance of CaH_6 and NbH_3 was investigated based on the density functional theory (DFT), which were chosen as the typical representative MSHCs due to their differences in structure and chemical bonding. The critical influences on energetic performance imposed by the structures of MSHCs were uncovered. Further investigations reveal that CaH_6 also possesses high energy density and high specific impulse, highlighting its potential applications as high explosives and propellant components.

2. Methods

The original structures of CaH_6 and NbH_3 under high pressure are obtained from experimental data,[20,22] and are investigated using the Vienna *Ab Initio* Simulation Package (VASP)[27,28] afterwards. The projector augmented wave (PAW) method[29] with a plane-wave cutoff energy of 400 eV is employed, and the Perdew–Burke–Ernzerhof (PBE) functional within the generalized gradient approximation (GGA)[30] is used to describe the exchange–correlation interactions. Considering the strong electron correlation effects in NbH_3, the Hubbard parameter U[31] is applied to the effective potential. The effective U value is set to 2.0 eV for d-orbitals of Nb atoms, as used in the previous literature.[32] To account for van der Waals interactions, the DFT-D3 method[33] is applied for corrections. The convergence criteria for the Hellmann–Feynman force and energy are set to 0.01 eV/Å and 1×10^{-5} eV, respectively. The K-point mesh is sampled within $2\pi\times0.02$ Å^{-1} using the Gamma scheme in the Brillouin zone. The structures and electron localization function (ELF) of the two MSHCs are visualized using the VESTA ver. 3.90.0a program.[34] The integrated crystalline orbital Hamiltonian population (ICOHP) calculations are carried out by employing the LOBSTER ver.5.1.1 program.[35]

The calculations of the theoretical detonation parameters of the two high-pressure MSHCs, including heat of detonation (Q), detonation velocity (D), and detonation pressure (P), were conducted following the Hess's law and Kamlet–Jacobs equations[36] as shown below:

$$Q = E(M) + \frac{x}{2}E(H_2) - E(MH_x), \tag{1}$$

$$\phi = 0.4885 N m^{\frac{1}{2}} Q^{\frac{1}{2}}, \tag{2}$$

$$D = 1.01\phi^{\frac{1}{2}}(1+1.30\rho), \tag{3}$$

$$P = 1.558\phi\rho^2, \tag{4}$$

where M = Ca and Nb, and x = 6 and 3, respectively; ϕ represents a parameter for energy under detonation conditions, N (in mol/g) represents the amount of moles of gas products formed per gram of MSHCs during detonation under high pressure, m is the average molar mass of these gases, which is 2.016 g/mol, and ρ (in g/cm^3) denotes the density of the two MSHCs under high pressure. Moreover, the energy densities of the two MSHCs are numerically equal to their Q, according to the common definition for traditional energetic materials.

The thermal decomposition behavior of CaH_6 was simulated by AIMD within the CP2K program,[37] with the orbital transformation technology[38] used to accelerate computing. A $2\times2\times2$ supercell of CaH_6 containing 112 atoms was conducted and optimized under 200 GPa. After optimization, the system was run for 10 ps at 3000 K, and subsequently for 3 ps with cooling to 298.15 K in the constant NPT ensemble at 1 atm under the PBE-D3[39] level of theory with the DZVP-MOLOPT-SR-GTH[40] basis set. The convergence criteria for forces and energy were set to 0.01 eV/Å and 1×10^{-5} eV, respectively. All simulations were performed under periodic boundary conditions (PBC), and the thermostat was set as CSVR for efficient and accurate temperature control. The time step was 0.5 fs, and the time constant was 200 fs. The DIIS minimizer was employed for all integration calculations in the simulations.

The calculations of combustion performance were carried out by employing the Explo5 ver.6.04 program under isobaric combustion conditions at a chamber pressure of 7 MPa, with equilibrium expansion conditions at the nozzle throat.

3. Results and discussion

3.1. Structures and bonding features

In this study, CaH_6 and NbH_3 were chosen and investigated as examples of MSHCs by employing the first-principle GGA-PBE method. Firstly, CaH_6 and NbH_3 were optimized respectively under 150 GPa and 300 GPa. The calculated structures are similar to the experimental structures,[20,22] and all the relative errors in lattice parameters are within 5% (as listed in Table S1), indicating the reliability of our computational scheme. High formation pressure always causes the

energy input to systems, and the energy properties of CaH_6 and NbH_3 are closely related to the programmed pressure. To eliminate the impact of different programmed pressures, we optimized both structures again at 200 GPa. The structures of CaH_6 and NbH_3 under 200 GPa almost remain unchanged, and the detailed structure parameters are listed in Table S2. All following discussions of the structures, energies and properties of CaH_6 and NbH_3 are based on the structures at 200 GPa.

As shown in Figs. 1(a) and 1(b), compared to ambient-pressure metal hydrides, MSHCs always have higher H coordination, more complex geometric structures and novel electronic configurations. Besides the interactions between metal and H atoms, the high pressure facilitates to drive the transformation of hydrogen to atomic phases. The H sublattices in MSHCs always feature a strong covalent H–H network and high electron density. We first discuss the geometric structures of CaH_6 and NbH_3.

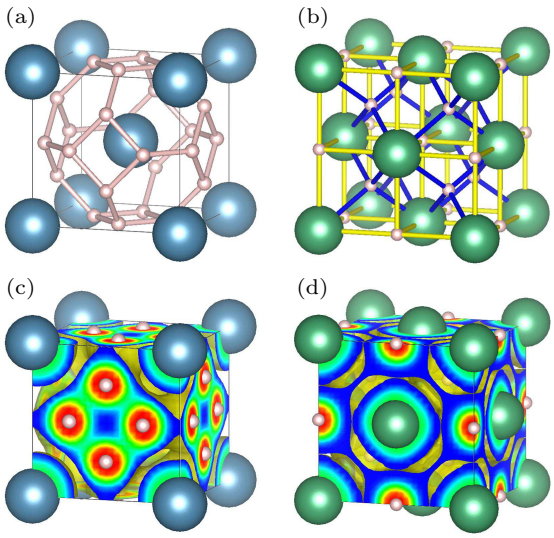


Fig. 1. Structures and ELF of high-pressure MSHCs. (a) The structure of CaH_6 under 200 GPa. (b) The structure of NbH_3 under 200 GPa. (c) The ELF (isosurface = 0.1) of CaH_6 under 200 GPa. (d) The ELF (isosurface = 0.1) of NbH_3 under 200 GPa. The white, blue, and green balls represent the H, Ca, and Nb atoms, respectively. The pink, blue and yellow bonds represent the H–H covalent bonds in CaH_6, the Nb–H_{Y-type} and Nb–H_{Z-type} bonds in NbH_3, respectively. The Ca–H bonds are not presented.

Under 200 GPa, the structure of CaH_6 (shown in Fig. 1(a)) exhibits high symmetry and high hydrogen content. The Ca atoms in CaH_6 form body-centered cubic (BCC) sublattices, and the uniformly distributed H atoms form a highly symmetric covalent H network. Specifically, each H atom bonds with four adjacent H atoms via equivalent H–H covalent bonds with a bond length of 1.191 Å. Every 24 H atoms constitute a H_{24} cage, in which eight H_6 hexagonal units are located in the tetrahedral interstitial sites and six H_4 square units are located in the octahedral interstitial sites of the Ca sublattice. In addition, all the distances from the H atoms to the cage-centered Ca atoms in CaH_6 are 1.883 Å.

NbH_3 (shown in Fig. 1(b)) has an XY_2Z-type Heusler structure, where the Nb atoms occupy the X sites in a face-centered cubic (FCC) arrangement and the H atoms occupy the Y and Z sites. The Y-type and Z-type H atoms in NbH_3 are individually distributed in the tetrahedral and octahedral interstitial sites of the Nb sublattice, respectively. The bond lengths of Nb–H_{Y-type} bond and Nb–H_{Z-type} bond are respectively 1.719 Å and 1.985 Å, and the shortest distance between the adjacent H atoms is 1.719 Å.

Further, the electronic structure and bonding features of CaH_6 and NbH_3 were investigated via ELF and ICOHP. The ELF, derived from the topological analysis of electron pair probability based on the Pauli exclusion principle, can intuitively display the electron occupation in the MSHCs system.[41] And the ICOHP values (commonly negative) can be used to evaluate the interaction strengths between two atoms by integrating the partition of band–structure energy calculated via the Hamiltonian matrix elements weighted densities of states. Specifically, the lower ICOHP value indicates the stronger interaction, while the value close to zero implies no chemical bonding.[42,43]

The ELF of CaH_6 (shown in Fig. 1(c)) shows that there is low electron occupation around Ca atoms and higher electron occupation around H atoms, which implies the electron delocalization and metallization of CaH_6. Notably, relatively high electron occupation exists between the adjacent H atoms and expands in the H sublattice of CaH_6, which implies an extended H network with covalent H–H bonds. The ICOHP value for H–H bonds (−0.559 eV) is lower than those for Ca–H (−0.126 eV) and Ca–Ca (−0.036 eV) interactions. Both ELF and ICOHP of CaH_6 reveal the strong H–H covalent bonding, weak interaction between Ca and H atoms and no interaction between Ca atoms.

For NbH_3 (shown in Fig. 1(d)), the ICOHP values of Nb–H_Y, Nb–H_Z and Nb–Nb are respectively −1.201 eV, −0.585 eV and −0.534 eV, which imply the strong bonding interactions of Nb–H and Nb–Nb. The high electron occupation between the Nb and H atoms indicates that Nb–H bonds exhibit a certain degree of covalent character, and both the low electron occupation and the near-zero ICOHP value of −0.040 eV between the adjacent H atoms indicate the weak interactions between them.

Here, we further discuss the performance of H atoms under different pressures. Under ambient pressure, H atoms typically form H_2 molecules, where the H–H bond is a σ-bond formed by the overlap of the two 1s orbitals of H atoms, with a bond length of 0.74 Å and an ICOHP value of −2.555 eV. The intermolecular distances between H_2 molecules exceed 3 Å, and their interactions are dominated by dispersion forces. For the traditional metal hydrides at ambient-pressure conditions, such as AlH_3, H atoms interact with metal atoms through ionic

bonds, while there is almost no interaction between H atoms. The ELF (Fig. S1) and ICOHP of AlH_3 indicate that electron occupation mainly locates around H atoms. The ICOHP values for Al–H and H–H are respectively −1.309 eV and −0.003 eV, which means the strong ionic interactions between Al and H atoms but almost no interactions between H atoms.

However, the H atoms behave differently in high-pressure MSHCs. The high pressure increases both the potential energy and kinetic energy of CaH_6 and NbH_3 systems, and the kinetic energy increases more quickly than the Coulomb energy with the increase of pressure.[44] The increase of kinetic energy closely depends on the growth rates of pressure and intrinsic properties of the systems, which causes the electron delocalization and metallization of the atoms. Different performances of metallization occur in high-pressure CaH_6 and NbH_3, which is ascribed to their different metal atoms and other inherent properties. For the CaH_6 system, under 200 GPa, the electronic delocalization of Ca and H atoms causes the formation of the equivalent covalent bonding between the H atoms. These pressure-induced delocalized covalent H–H bonds are weaker than the typical σ-bond in the H_2 molecule, which aids in forming the metastable covalent H network. This extended H sublattice in CaH_6 is a metallic-hydrogen-like structure featuring high energy density. In the NbH_3 system, electron delocalization causes a certain degree of covalent character in Nb–H bonds and strong bonding between Nb atoms.

3.2. Energetic performance

The above discussion suggests that the MSHCs possess high energy. In the following section, the energetic performance of CaH_6 and NbH_3 has been well studied. Also, the relationship between their structural characteristics and energetic performance was explored theoretically by using thermodynamic and molecular dynamics methods.

3.2.1. Basic properties

The energetic performance of energetic materials is closely related to their density, formation enthalpy and energy density. Higher density, higher positive formation enthalpy and higher energy density generally contribute to better energetic performance of explosives.[45] The densities (ρ), formation enthalpies (ΔH_f) and energy density (E_d, numerically equal to detonation heat, Q) of CaH_6 and NbH_3 under 200 GPa were calculated and listed in Table 1.

The ρ of CaH_6 and NbH_3 under 200 GPa are 4.01 g/cm^3 and 10.08 g/cm^3, respectively. The high ρ of MSHCs is attributed to the high compact crystal structure compressed by high pressure and the inherent high mass of metal atoms. Their ΔH_f values are respectively 1020.98 kJ/mol and 468.92 kJ/mol, both higher than that of CL-20, whose ΔH_f is a high positive value of 377 kJ/mol. CaH_6 possesses a higher E_d of 22.13 kJ/g, which is 3.6 times that of CL-20 (a traditional energetic material, whose E_d is 6.56 kJ/g) and 2.3 times that of cubic gauche polymeric nitrogen (cg-N, a novel high-pressure energetic material, whose E_d is 9.7 kJ/g).[50] While, the E_d of NbH_3 is comparable to that of TNT (4.184 kJ/g[46]) but below CL-20. The outstanding E_d value of CaH_6 is closely related to its structure and chemical bonding. CaH_6 has a metallic-hydrogen-like structure with high H coordination and extended covalent H–H bonding induced by high pressure. This unique structure makes CaH_6 in the metastable state and tends to store more energy introduced by high pressure within the H networks in the form of chemical energy. In contrast, NbH_3 lacks the metallic-hydrogen-like structure and bonding features resembling CaH_6. Most of the energy introduced by high pressure is stored in the form of Coulomb energy. As a result, NbH_3 has a relatively low E_d compared to CaH_6.

Table 1. Properties of high-pressure MSHCs.

Compound	Basic properties		Detonation performance			
	ρ (g/cm^3)	ΔH_f (kJ/mol)	N (mol/g)	Q (E_d) (kJ/g)	D (km/s)	P (GPa)
$CaH_6^{ideal\ (a)}$	4.01	1020.98	0.0650	22.13	16.25	168.95
$CaH_6^{MD\ (b)}$	4.01	1020.98	0.0474	9.51	11.23	80.25
$NbH_3^{ideal\ (a)}$	10.18	468.92	0.0156	4.89	12.52	122.54
CL-20$^{pre.\ (c)}$	2.04	377	0.0308	6.56	9.62	44.1
CL-20$^{exp.\ (c)}$	2.04	377.4 ± 13	–	6.1	9.6	43

(a) Parameters calculated based on the ideal case, (b) parameters calculated based on the MD simulation results, (c) predicted (via K–J equations) and experimental parameters for CL-20, Refs. [46–49]. Densities (ρ), formation enthalpies (ΔH_f), energy density (E_d, numerically equal to detonation heat, Q), gas production (N), theoretical detonation heat (Q), detonation velocity (D), and detonation pressure (P) are all included.

3.2.2. Detonation performance

The K–J equations are a common method for predicting the detonation parameters of traditional CHON-based energetic materials, which have also been employed for metal-containing systems.[51] Here, we also borrowed the K–J equations to describe the detonation performance of MSHCs to a certain extent. The detonation parameters are closely related to the detonation reaction process and the corresponding final products. In an ideal case, the final products consist of metal crystal and H_2 gas, in which the energy release reaches its optimal level. The corresponding detonation parameters were calculated and listed in Table 1, including the gas production (N), theoretical detonation heat (Q), detonation velocity (D), and detonation pressure (P).

The N of CaH_6 and NbH_3 are respectively 0.0650 mol/g and 0.0145 mol/g, due to the difference in their hydrogen content. The Q (numerically equal to E_d) of CaH_6 and NbH_3 are respectively 5.3 times and 1.2 times TNT equivalent, and all

values for their D and P are higher than those of CL-20. Particularly, both the D and P of CaH_6 are higher than those of NbH_3 by over 30%, which is primarily attributed to its larger H content and the extra energy stored in its metallic-hydrogen-like structure, as discussed above. Thus, substantial amounts of high-temperature gases are released during its detonation, which provides the necessary force for working.

3.3. Decomposition behavior of CaH_6

As discussed above, CaH_6 possesses metallic-hydrogen-like H–H covalent bonds and superior detonation performance. In this section, we further explored its energetic performance and potential applications by employing the *ab initio* molecular dynamics (AIMD) method and CP2K software. The decomposition process was theoretically simulated with a CaH_6 model containing 112 atoms. The system was first optimized under 200 GPa and then was simulated for 3 ps within the NVT ensemble. To provide sufficient energy to initiate the decomposition, the thermostat temperature was set to 3000 K. The evolution of the potential energy and the structure throughout the decomposition simulation are shown in Fig. 2.

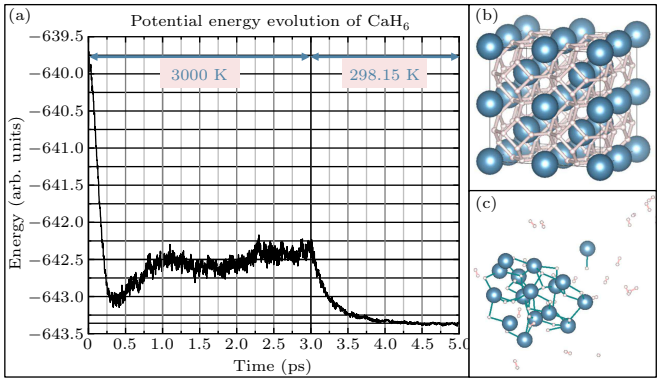


Fig. 2. Decomposition behavior of high-pressure CaH_6. (a) The potential energy evolution of the decomposition of CaH_6. (b) The structure of CaH_6 before decomposition. (c) The products of the decomposition of CaH_6. The blue and white balls represent the Ca and H atoms, respectively. The pink and green bonds represent the H–H and Ca–H bonds, respectively.

After short time heating, the CaH_6 system undergoes a rapid decomposition stage within 0.4 ps. During this stage, extensive bond dissociation occurs, accompanied by the release of hydrogen atoms and a sharp decline in potential energy. The freed H atoms further bond with neighboring H or Ca atoms to form H_2 and Ca_nH_m clusters. At the end of this stage, 73% of H atoms form H_2 molecules and the remaining 27% participate in the formation of Ca_nH_m clusters, as shown in Fig. 2(c). According to this simulated decomposition process, there is a decrease in both energy release and detonation parameters of CaH_6 compared to the ideal case. Based on the potential energy decline throughout the simulations, the detonation parameters (denoted as CaH_6^{MD}) were calculated and listed in Table 1. The results show that CaH_6 exhibits large gas production ($N^{MD} = 0.0474$ mol/g, or 1062.26 mL/g), also far exceeding that of CL-20 (628.5 mL/g.[52]). The Q^{MD} is 9.51 kJ/g, which is 2.3 times that of TNT. The D^{MD} and P^{MD} are 11.23 km/s and 80.25 GPa, respectively. Consequently, Table 1 shows the detonation performance of CaH_6 in different decomposition processes, the N, Q, D and P respectively lie in (0.65–0.474 mol/g), (22.13–9.51 kJ/g), (16.25–11.23 km/s) and (168.95–80.25 GPa), which are all higher than those of CL-20. Our simulation validates the excellent detonation performance of CaH_6 and its tremendous potential as high explosives.

The above discussion about the hydrogen release suggests the potential of CaH_6 for high-performance propellant component. Further, its combustion performance was predicted by using the Explo 5 software. The theoretical vacuum specific impulse (I_{sp}) of CaH_6 is 490.66 s, which is 1.9 times that of hexogen (RDX, whose I_{sp} is 258 s)[53] and 3.2 times that of ammonium perchlorate (AP, whose I_{sp} is 155 s).[54] The characteristic velocity (c^*) and the combustion temperature of CaH_6 are 2672.4 m/s and 2620.7 K, respectively. The main combustion products consist of 24.54% Ca and 71.76% H_2, corresponding to a hydrogen release ratio of 97.48%. All these results highlight that high-pressure CaH_6 exhibits combustion performance far exceeding that of common high-energy propellant components such as RDX and AP, suggesting its potential for propellants.

4. Conclusion

For the first time, CaH_6 and NbH_3 were chosen as examples of MSHCs to systematically investigate their energetic performance. Since the two MSHCs were obtained under high pressure, both the potential and kinetic energy of the systems increase, while the increase in kinetic energy is more rapid than the Coulomb energy as the pressure rises. Consequently, both MSHCs exhibit high energy densities, with the values of 5.3 times and 1.2 times that of TNT, respectively. Notably, the outstanding energy density of CaH_6 is relatively higher than that of NbH_3, which is closely related to the structure and characteristic H–H covalent bonds in CaH_6. CaH_6 possesses highly ordered extended H sublattice and metastable covalent H network with strong pressure-induced covalent H–H bond, which are similar to those in metallic hydrogen and offer CaH_6 higher energy density.

Given this, we conducted an in-depth study of its detonation process and energy release performance. First of all, instead of the complete decomposition into pure Ca metal and H_2, CaH_6 might undergo complex reactions and produce various Ca_nH_m clusters. Furthermore, the corresponding energy density of CaH_6 was predicted as 2.3 times TNT equivalent. Consequently, the theoretical energy density of CaH_6 ranges from 2.3 to 5.3 times TNT equivalent. Moreover, at least 72.9% of H atoms in CaH_6 are finally released to form 35

H_2 molecules in the rapid energy-release stage, suggesting its potential for high-performance propellant component. Therefore, we further predicted its combustion performance. The theoretical specific impulse, characteristic velocity and hydrogen release ratio of CaH_6 are respectively 490.66 s, 2672.4 m/s and 97.48%, indicating its superior combustion performance far exceeding that of common high-energy propellant components such as RDX and AP.

Our results demonstrate that the energy density and energy release of high-pressure MSHCs are significantly higher than traditional CHON-based explosives, which makes them a promising candidate for next-generation energetic materials. Certain high-pressure MSHCs, such as CaH_6, possess metallic-hydrogen-like structures and characteristic covalent bonds and can release substantial amounts of high-temperature gases during their detonation, demonstrating tremendous potential for explosives and high-energy propellant components. To date, stabilizing MSHCs, which are synthesized at high pressure, under ambient pressure conditions is very challenging. Using the pressure-quench protocol (PQP) or achieving solid solutions is promising to recover the pressure-induced phases to ambient pressure, which may extend the research on MSHCs from basic studies to applied research. This study enhanced the chemical understanding of MSHCs and provided a new route to design novel high-energy-density materials, promoting the exploration of MSHCs in defense, aerospace, and energy sectors.

References

[1] Wigner E and Huntington H 1935 *The Journal of Chemical Physics* **3** 764
[2] Ashcroft N W 1968 *Phys. Rev. Lett.* **21** 1748
[3] Nellis W 1999 *Philosophical Magazine B* **79** 655
[4] Isaac F S and John W C 2010 *J. Phys.: Conf. Ser.* **215** 012194
[5] McMahon J M and Ceperley D M 2011 *Phys. Rev. B* **84** 144515
[6] Dias R P and Silvera I F 2017 *Science* **355** 715
[7] Ashcroft N 2004 *Phys. Rev. Lett.* **92** 187002
[8] Duan D, Liu Y, Tian F, Li D, Huang X, Zhao Z, Yu H, Liu B, Tian W and Cui T 2014 *Scientific Reports* **4** 6968
[9] Drozdov A, Eremets M, Troyan I, Ksenofontov V and Shylin S I 2015 *Nature* **525** 73
[10] Abe K 2017 *Phys. Rev. B* **96** 144108
[11] Somayazulu M, Ahart M, Mishra A K, Geballe Z M, Baldini M, Meng Y, Struzhkin V V and Hemley R J 2019 *Phys. Rev. Lett.* **122** 027001
[12] Ma L, Wang K, Xie Y, Yang X, Wang Y, Zhou M, Liu H, Yu X, Zhao Y and Wang H 2022 *Phys. Rev. Lett.* **128** 167001
[13] Luo Y X, Gao J, Liu Q J, Fan D H and Liu Z T 2024 *Journal of Molecular Modeling* **30** 229
[14] Miao M, Sun Y, Zurek E and Lin H 2020 *Nature Reviews Chemistry* **4** 508
[15] Sun Y and Miao M 2023 *Chem* **9** 443
[16] Tarasov B P, Bocharnikov M S, Yanenko Y B, Fursikov P V, Minko K B and Lototskyy M V 2020 *J. Phys.: Energy* **2** 024005
[17] Wu X L, Xu S, Pang A M, Cao W G, Liu D B, Zhu X Y, Xu F Y and Wang X 2021 *Defence Technology* **17** 1262
[18] Bezdudny A, Blinov D and Dunikov D 2023 *Journal of Energy Storage* **68** 107590
[19] Makhov M 2024 *Russian Journal of Physical Chemistry B* **18** 185
[20] Li Z, He X, Zhang C, Wang X, Zhang S, Jia Y, Feng S, Lu K, Zhao J and Zhang J 2022 *Nat. Commun.* **13** 2863
[21] He X, Zhang C, Li Z, Zhang S, Min B, Zhang J, Lu K, Zhao J, Shi L and Peng Y 2023 *Chin. Phys. Lett.* **40** 057404
[22] He X, Zhang C, Li Z, Lu K, Zhang S, Min B, Zhang J, Shi L, Feng S and Liu Q 2024 *Materials Today Physics* **40** 101298
[23] Banacky P and Noga J 2021 *J. Appl. Phys.* **130** 183902
[24] Hou P, Huo Z and Duan D 2023 *The Journal of Physical Chemistry C* **127** 23980
[25] Denchfield A, Park H and Hemley R J 2024 *Proc. Natl. Acad. Sci. USA* **121** e2413096121
[26] Sun Y, Zhong X, Liu H and Ma Y 2024 *National Science Review* **11** nwad270
[27] Kresse G and Furthmuller J 1996 *Computational Materials Science* **6** 15
[28] Kresse G and Furthmuller J 1996 *Phys. Rev. B* **54** 11169
[29] Blochl P E 1994 *Phys. Rev. B* **50** 17953
[30] Perdew J P, Burke K and Ernzerhof M 1996 *Phys. Rev. Lett.* **77** 3865
[31] Dudarev S L, Botton G A, Savrasov S Y, Humphreys C and Sutton A P 1998 *Phys. Rev. B* **57** 1505
[32] Solovyev I V, Dederichs P H and Anisimov V I 1994 *Phys. Rev. B* **50** 16861
[33] Grimme S, Antony J, Ehrlich S and Krieg H 2010 *The Journal of Chemical Physics* **132** 154104
[34] Momma K and Izumi F 2011 *Journal of Applied Crystallography* **44** 1272
[35] Maintz S, Deringer V L, Tchougreeff A L and Dronskowski R 2016 *Journal of Computational Chemistry* **37** 1030
[36] Kamlet M J and Jacobs S 1968 *The Journal of Chemical Physics* **48** 23
[37] Hutter J, Iannuzzi M, Schiffmann F and VandeVondele J 2014 *Wiley Interdisciplinary Reviews: Computational Molecular Science* **4** 15
[38] VandeVondele J and Hutter J 2003 *The Journal of Chemical Physics* **118** 4365
[39] Zhao D, Liu S, Rong C, Zhong A and Liu S 2018 *ACS Omega* **3** 17986
[40] VandeVondele J and Hutter J 2007 *The Journal of Chemical Physics* **127** 114105
[41] Chesnut D B 2000 *The Journal of Physical Chemistry A* **104** 11644
[42] Dronskowski R and Blochl P E 1993 *The Journal of Physical Chemistry* **97** 8617
[43] Deringer V L, Tchougreeff A L and Dronskowski R 2011 *The Journal of Physical Chemistry A* **115** 5461
[44] Ashcroft N W, Mermin N D and Rodriguez S 1978 *American Journal of Physics* **46** 116
[45] Robertson R 1921 *Journal of the Chemical Society, Transactions* **119** 1
[46] Meyer R, Kohler J and Homburg A 2016 *Explosives* 7th Ed. (Weinheim: Wiley-VCH)
[47] Politzer P and Murray J S 2011 *Central European Journal of Energetic Materials* **8** 209
[48] Simpson R, Urtiew P, Ornellas D, Moody G, Scribner K and Hoffman D 1997 *Propellants, Explosives, Pyrotechnics* **22** 249
[49] Muravyev N V, Monogarov K A, Melnikov I N, Pivkina A N and Kiselev V G 2021 *Physical Chemistry Chemical Physics* **23** 15522
[50] Yin K, Wang Y, Liu H, Peng F and Zhang L 2015 *Journal of Materials Chemistry A* **3** 4188
[51] Huang B, Wang B, Wu S, Guogan F, Hu W and Frapper G 2021 *Chemistry of Materials* **33** 5298
[52] He S, Zhang L, Heng S, Liu Z and Shi Z 2007 *Energetic Materials* **15** 515
[53] Liu D, Chen J, Yang R, Xiao L, Zhang G, Feng X, Zhang K, Jiang W and Hao G 2024 *Chemistry of Materials* **36** 3496
[54] Klapotke T M 2018 *Energetic Materials Encyclopedia* (Berlin: De Gruyter)